Symmetry and dynamics universality of supermetal in quantum chaos

Ping Fang,[1] Chushun Tian,[2,*] and Jiao Wang[1,†]

[1]*Department of Physics and Institute of Theoretical Physics and Astrophysics, Xiamen University, Xiamen 361005, Fujian, China*

[2]*Institute for Advanced Study, Tsinghua University, Beijing 100084, China*

(Dated: December 31, 2015)

Chaotic systems exhibit rich quantum dynamical behaviors ranging from dynamical localization to normal diffusion to ballistic motion. Dynamical localization and normal diffusion simulate electron motion in an impure crystal with a vanishing and finite conductivity, i.e., an "Anderson insulator" and a "metal", respectively. Ballistic motion simulates a perfect crystal with diverging conductivity, i.e., a "supermetal".We analytically find and numerically confirm that, for a large class of chaotic systems, the metal-supermetal dynamics crossover occurs and is universal, determined only by the system's symmetry. Furthermore, we show that the universality of this dynamics crossover is identical to that of eigenfunction and spectral fluctuations described by the random matrix theory.

PACS numbers: 05.45.Mt, 64.70.Tg

arXiv:1510.01241v2 [nlin.CD] 30 Dec 2015

I. INTRODUCTION

Chaotic systems exhibit a wealth of quantum phenomena. A canonical example is the quantum kicked rotor [1] (see Refs. [2–4] for reviews)—a free rotating particle under the influence of sequential time-periodic driving, the Hamiltonian of which reads

$$\hat{H} = \frac{1}{2}(\tilde{h}\hat{n})^2 + K\cos\hat{\theta}\sum_m \delta(t-m). \tag{1}$$

Here the time t is rescaled by the kicking period τ, the Planck's quantum $\tilde{h} = \hbar\tau/I$ with I the particle's moment of inertia, and the angular momentum $\hat{n}$ canonically conjugates to the angular position θ. The dimensionless amplitude of the kicking potential, K, namely the so-called classical stochastic parameter, governs the degree of the system's nonlinearity. Despite this seemingly simple construction, tuning $\tilde{h}$ gives rise to rich dynamical behaviors. For example, for (generic) irrational values of $\tilde{h}/(4\pi)$ the rotor's kinetic energy saturates at long times [18], in sharp contrast to the linear energy growth in the classical limit of vanishing $\tilde{h}$ [5]. The former, the so-called dynamical localization, simulates an Anderson insulator [6] while the latter simulates a (normal) metal. Even more striking, $\tilde{h}$-driven phenomena occur to variants of the kicked rotor and they simulate a broad spectrum of condensed-matter systems (e.g., Refs. [7–15]). Most recently, it has been found that for a spinful quasiperiodically kicked rotor, the Planck's quantum can drive a sequential rotor Anderson insulator-metal transition shown to be the mathematical equivalence of the integer quantum Hall effect [16].

A peculiar phenomenon common to various kicked rotor systems is the so-called quantum resonance for rational values of $\tilde{h}/(4\pi) = p/q$, with p and q being coprime natural numbers [17]. For these values of $\tilde{h}$ the rotor's kinetic energy grows quadratically at large times, which is much faster than the metallic (linear) growth. Such a phase simulates a perfect crystal with diverging electric conductivity corresponding to ballistic electron motion. Therefore, it is dubbed "supermetal". Physically, for rational $\tilde{h}/(4\pi)$ the system exhibits translation symmetry in the angular momentum space, and resonant transmission through the ensuing Bloch bands gives rise to the supermetallic (quadratic) growth. The extreme sensitivity of the system's behavior such as dynamical localization and quantum resonance to the number-theoretic property of $\tilde{h}/(4\pi)$ is a prominent feature that distinguishes the kicked rotor from genuine disordered systems (see Refs. [2, 12, 18–23] for reviews of the early and recent status of this subject). Over decades, this subject has been central to theoretical and experimental studies of quantum chaos. Recently, the supermetallic phase of the kicked rotor has been experimentally observed in chemical systems and finds potential applications such as achieving spin-selective rotational excitation of molecules [24].

So far, most studies have focused on the asymptotic supermetallic growth and are mute to effects of chaoticity. In Ref. [22], it is first found by using the field theory that for the standard kicked rotor the chaoticity gives rise to a universal crossover from metallic to supermetallic energy growth which is insensitive to the system's details such as the values of p and q and the strength of the kicking potential. Moreover, it has been found that this universal dynamical behavior has a deep connection to the optical conductivity of perfect crystals [25, 26] and the quantum walk in the periodic multi-baker map [27–29]. A fundamental question naturally arises: How robust is this dynamical behavior? Notably, it is unclear whether such dynamics universality exists in general periodic chaotic systems and is impervious to the symmetry. The present work aims at a systematic study of these issues.

We study the supermetallic phase (rational $\tilde{h}/(4\pi)$) of a large class of generalized kicked rotor systems. These

*Electronic address: ctian@mail.tsinghua.edu.cn

†Electronic address: phywangj@xmu.edu.cn

systems have qualitatively different dynamical behaviors (e.g., dynamical localization or delocalization) when $\tilde{h}/(4\pi)$ is irrational. We analytically show and numerically confirm that chaoticity leads to even richer universal behavior in the crossover from metallic to supermetallic energy growth. We find that the universal dynamics crossover behavior is very sensitive to the symmetry of the Hamiltonian describing the free rotation of the particle, but not to system's details. We show that the universal metal-supermetal dynamics crossover can be attributed to the universality of fluctuations of the Bloch wave functions and bands of the reduced quantum system in a unit cell. The latter motivates us to conjecture that the universality class of supermetal dynamics is identical to that of eigenfunction and spectral fluctuations described by the random matrix theory (RMT) [30].

The rest of the paper is organized as follows. In the next section we introduce the models and discuss their symmetries. We present the analytical results of the energy growth in Sec. III and put them to numerical test in Sec. IV. In Sec. V we discuss the RMT foundation of the universality of supermetal dynamics. We conclude in Sec. VI. Some technical details are presented in Appendix A.

II. MODEL AND SYMMETRY

In this work we will explore the dynamical behavior of a large class of generalized quantum kicked rotors for rational values of $\tilde{h}/(4\pi)$. In this section we first describe the models and discuss their symmetries.

A. Generalized quantum kicked rotor

The system to be considered below has a general Hamiltonian as follows,

$$\hat{H} = H_0(\hat{n}) + K\cos\hat{\theta}\sum_m \delta(t-m). \tag{2}$$

Here we assume the free rotation Hamiltonian $H_0(\hat{n})$ to be an analytic function of $\hat{n}$ which can be expressed as

$$H_0(\hat{n}) = \sum_{k=0}^{\infty} c_k \hat{n}^k, \tag{3}$$

where the numerical coefficients c_k generally depend on $\tilde{h}$. The angular momentum operator $\hat{n}$ canonically conjugates to the angular operator $\hat{\theta}$ and has the eigenvalue spectrum $\{\tilde{n}\}, \tilde{n} \in \mathbb{Z}$. When $H_0(\hat{n}) = \frac{1}{2}\tilde{h}^2\hat{n}^2$ the system is reduced to the standard quantum kicked rotor (1). The quantum evolution can be expressed as a stroboscopic dynamics such that the wave vector at integer time t, $|\psi(t)\rangle$, is given by

$$|\psi(t)\rangle = \hat{U}^t|\psi(0)\rangle, \quad t \in \mathbb{Z}, \tag{4}$$

with the Floquet operator

$$\hat{U} = e^{-\frac{i}{2\tilde{h}}H_0} e^{-\frac{iK}{\tilde{h}}\cos\hat{\theta}} e^{-\frac{i}{2\tilde{h}}H_0}. \tag{5}$$

As mentioned above, we shall focus on $\tilde{h}/(4\pi) = p/q$ throughout this work.

B. Symmetry

First of all, we shall consider such c_k that $H_0/\tilde{h}$ is shifted by multiple 2π upon the translation operation

$$\hat{T}_q: \quad \hat{n} \to \hat{n} + q. \tag{6}$$

As a result,

$$[\hat{U}, \hat{T}_q] = 0, \tag{7}$$

implying that the system exhibits the translation symmetry in the $\hat{n}$ space. This brings the rotor to the supermetallic phase.

Next, the system exhibits an effective time-reversal symmetry. To be specific, we note that the Hamiltonian (2) is invariant under the 'time-reversal' operation

$$\hat{T}_c: \quad \hat{n} \to \hat{n},\ \hat{\theta} \to -\hat{\theta},\ t \to -t. \tag{8}$$

This has an important consequence, i.e.,

$$\hat{U}^{\mathcal{T}} = \hat{U}, \tag{9}$$

where the superscript '$\mathcal{T}$' stands for the transpose. This $\hat{T}_c$ symmetry brings the system to the orthogonal class in the RMT.

Finally, if $c_k = 0$ for all odd k, then $H_0(\hat{n})$ and thereby the system bears an additional symmetry, i.e., $\hat{U}$ being invariant under the operation

$$\hat{T}_i: \quad \hat{n} \to -\hat{n}. \tag{10}$$

Otherwise this symmetry is broken. This symmetry is dubbed the "inversion symmetry" following solid-state physics [31]. Its effects on the quantum resonance have not yet been explored [32] and this is the main subject of this work.

III. THEORY OF SUPERMETAL DYNAMICS

In this section we present an analytic theory for dynamics of a generalized quantum kicked rotor at resonance, i.e., the supermetallic phase. Particular attentions are paid to effects of the inversion symmetry. Armed with this theory, we explicitly calculate the rotor's 'kinetic energy' [33]

$$E(t) \equiv \frac{1}{2}\langle\psi(t)|\hat{n}^2|\psi(t)\rangle. \tag{11}$$

Throughout, to simplify technical discussions without loss of generality, we assume that the initial state is an unperturbed eigenstate with zero angular momentum, i.e., $|\psi(0)\rangle = |0\rangle$.

A. Reduced system

First of all, the quantum dynamics (4) in the angular momentum space is determined by the quantum amplitude, $\langle\tilde{n}|\hat{U}^t|\tilde{n}'\rangle$. It is easy to show that the time Fourier transformations of this amplitude and its complex conjugate, denoted as $\langle\tilde{n}|(1-e^{i\omega_+}\hat{U})^{-1}|\tilde{n}'\rangle$ and $\langle\tilde{n}'|(1-e^{-i\omega_-}\hat{U}^\dagger)^{-1}|\tilde{n}\rangle$, respectively, give

$$E(t) = \frac{1}{2}\sum_{\tilde{n}}\tilde{n}^2\int\frac{d\omega}{2\pi}e^{-i\omega t} \times \langle\langle\tilde{n}|(1-e^{i\omega_+}\hat{U})^{-1}|0\rangle\langle 0|(1-e^{-i\omega_-}\hat{U}^\dagger)^{-1}|\tilde{n}\rangle\rangle_{\omega_0}, \quad (12)$$

where $\omega_\pm=\omega_0\pm\frac{\omega}{2}$ and $\langle\cdot\rangle_{\omega_0}\equiv\frac{1}{2\pi}\int_0^{2\pi}d\omega_0$.

To proceed we consider the eigenvalues and eigenvectors of $\hat{U}$. The translation symmetry (7) entails a good quantum number, i.e., the Bloch angle $\theta\in[0,2\pi/q]$. According to Bloch's theorem,

$$\hat{U}|\psi_{\alpha,\theta}\rangle=e^{i\epsilon_\alpha(\theta)}|\psi_{\alpha,\theta}\rangle, \quad (13)$$

where both the quasienergy spectrum, $\{\epsilon_\alpha(\theta)\}$, and corresponding eigenvectors, $\{|\psi_{\alpha,\theta}\rangle\}$, depend on θ. The Bloch wave function

$$\psi_{\alpha,\theta}(\tilde{n})\equiv\langle\tilde{n}|\psi_{\alpha,\theta}\rangle=e^{i\tilde{n}\theta}\varphi_{\alpha,\theta}(\tilde{n}), \quad (14)$$

with $\varphi_{\alpha,\theta}(\tilde{n})$ being a q-periodic wave function,

$$\varphi_{\alpha,\theta}(\tilde{n})=\varphi_{\alpha,\theta}(\tilde{n}+q)=\varphi_{\alpha,\theta}(n). \quad (15)$$

In deriving the last equality of Eq. (15) we use the fact that $\tilde{n}$ can be uniquely written as $n+Nq$, where $0\le n\le q-1$ and $N\in\mathbb{Z}$. Upon applying Bloch's theorem to Eq. (12) we express the energy profile as

$$E(t)=-\frac{1}{2}\int\frac{d\omega}{2\pi}e^{-i\omega t}\sum_{n=0}^{q-1}\int_b d\theta_+\partial^2_{\theta_-}|_{\theta_-=\theta_+}K_\omega(n), \quad (16)$$

where the notation: $\int_b d\theta\equiv\frac{q}{2\pi}\int_0^{2\pi/q}d\theta$ has been introduced and

$$K_\omega(n) = \langle\langle n|\frac{1}{1-e^{i\omega_+}\hat{U}_{\theta_+}}|0\rangle \times \langle 0|\frac{1}{1-e^{-i\omega_-}\hat{U}^\dagger_{\theta_-}}|n\rangle\rangle_{\omega_0} \quad (17)$$

is the density correlation function for autonomous stroboscopic dynamics restricted on a circle of circumference q. This reduced system is governed by a θ-dependent Floquet operator,

$$\hat{U}_\theta=e^{-\frac{i}{2\hbar}H_0}e^{-\frac{iK}{\hbar}\cos(\hat{\theta}+\theta)}e^{-\frac{i}{2\hbar}H_0}. \quad (18)$$

Physically, $K_\omega(n)$ probes interference between retarded and advanced amplitudes corresponding to the reduced dynamics, and the Bloch angle θ introduces an "Aharonov-Bohm flux", $q\theta$, piercing through the circle (see Fig. 1). Note that the unitarity of $\hat{U}_\theta$ now implies $\sum_{n''=0}^{q-1}(\hat{U}_\theta)_{nn''}(\hat{U}^\dagger_\theta)_{n''n'}=\delta_{nn'}$ for arbitrary $n,n'\in\{0,1,\cdots,q-1\}$.

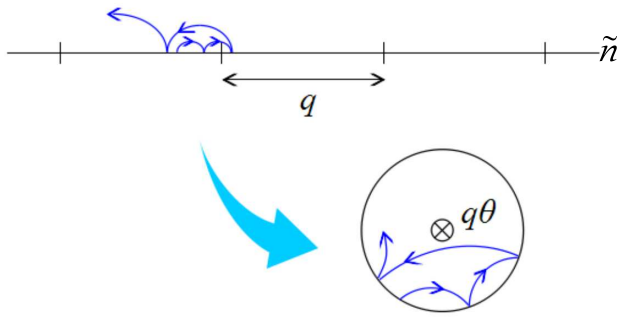

FIG. 1: (Color online) The translation symmetry entails a reduction of quantum dynamics from unbounded angular momentum space to a circle of circumference q pierced by an Aharonov-Bohm like flux $q\theta$ with θ being the Bloch angle.

It is important to note that for the reduced system governed by $\hat{U}_\theta$ the effective time-reversal symmetry $\hat{T}_c$ is broken by the Bloch angle if $\theta\neq 0,\pi$. A question naturally arises: Does this broken $\hat{T}_c$ symmetry bring the system to the unitary class in the RMT? As we will show in the following, the answer crucially depends on whether $H_0(\hat{n})$ exhibits the inversion symmetry $\hat{T}_i$. If the latter symmetry is broken, then the system belongs to the unitary class. If not, then $\hat{U}_\theta$ is invariant under the combined operation $\hat{T}_i\hat{T}_c$ and this brings the reduced system back to the orthogonal class.

B. Universal metal-supermetal dynamics crossover

1. *Field theory*

The remaining task is to calculate the two-particle Green's function $K_\omega(n)$ evaluated at fixed parameters $\theta_\pm$. Following Ref. [22] we may express it in terms of a functional integral,

$$K_\omega(n) = -\frac{1}{2^4}\int dQ\, e^{-S[Q]} \times \mathrm{str}\left(k(Q(n))_{+2,-2}k(Q(0))_{-2,+2}\right). \quad (19)$$

Here $Q\equiv\{Q_{\lambda\alpha\beta,\lambda'\alpha'\beta'}\}$ is a supermatrix defined on three sectors: the index $\lambda=+,-$ refers to the advanced and retarded ('AR') sector, $\alpha=f,b$ to the fermionic-bosonic ('FB') sector, and $\beta=1,2$ to the 'T' sector accommodating the symmetry under the combined operation $\hat{T}_i\hat{T}_c$; i.e., $\beta=1$ (2) refers to (in)variance under the $\hat{T}_i\hat{T}_c$ operation. Q satisfies the periodic boundary condition $Q(n)=Q(n+q)$. The constant matrix $k=\sigma^3_{\rm FB}\otimes\sigma^0_{\rm AR}\otimes\sigma^0_{\rm T}$, where $\sigma^0_{\rm X}$ is the unit (2×2) matrix

in the X sector. The action is given by

$$S = \frac{1}{2^4}\int_0^q dn \mathrm{str}\big(D_q(i\partial_n Q - [\hat{\vartheta}, Q])^2 - 2i\omega Q\sigma^3_{\mathrm{AR}}\big) \quad (20)$$

with

$$\hat{\vartheta} = \begin{pmatrix} \theta_+ & 0 \\ 0 & \theta_- \end{pmatrix}_{\mathrm{AR}} \otimes \sigma_{\mathrm{T}}^{-1+\beta^2} \otimes \sigma^0_{\mathrm{FB}}. \quad (21)$$

For $\beta = 2$ the matrix $\sigma_{\mathrm{T}}^{-1+\beta^2} = \sigma^3_{\mathrm{T}}$ represents the sign change in the Aharonov-Bohm flux under the $\hat{T}_c$ operation. The corresponding effective field theory has been obtained in Ref. [22], but for $\beta = 1$, an additional symmetry,

$$Q(n) = Q(q-n), \quad (22)$$

arises. Note that the above action is universal in the sense that it depends on system parameters only through the diffusion constant D_q. The effective field theory is valid, provided the parametric conditions, (i) $1 \ll K/\tilde{h} \ll q \ll (K/\tilde{h})^2$, (ii) $\omega \ll 1$, and (iii) $K \gg 1$ [34], are met. The physical meanings of these conditions are as follows. For (i), $K/\tilde{h}$ plays the role of the "transport mean free path" in normal metals; the inequality $K/\tilde{h} \ll q$ guarantees the validity of the hydrodynamic expansion, while $q \ll (K/\tilde{h})^2$ implies that localization physics does not play any roles. For (ii), means that we are concerned in time scales much larger than the kicking period. In (iii) and $K/\tilde{h} \gg 1$, it is implied that the angular (or more precisely, $\sin\hat{\theta}$) correlation rapidly decreases, i.e., strong chaoticity. The latter results in the fact that the distribution of the quasienergy spectrum $\{\epsilon_\alpha(\theta)\}$ of the Floquet operator $\hat{U}_\theta$ follows the Wigner-Dyson statistics for the circular orthogonal ensemble (COE) for $\beta = 1$ and the circular unitary ensemble (CUE) for $\beta = 2$.

In principle, the diffusion constant D_q depends on both the parameters K and $\tilde{h}$ and the details of H_0, i.e., c_k. The H_0 dependence arises from the short-time correlation contributions to the diffusion constant [22]. For $K/\tilde{h} \gg 1$ these correlation contributions are negligible and consequently only the parameter $(K, \tilde{h})$ dependence arises, i.e., $D_q = D_q(K, \tilde{h}) \sim (K/\tilde{h})^2$.

2. *Metallic-supermetallic growth crossover*

We proceed to use Eqs. (16), (19), and (20) to explicitly calculate $E(t)$. First of all, for $\omega \lesssim \Delta \equiv 2\pi/q$ which is the mean level spacing of the unit cell, the effective action (20) shows that inhomogeneous Q-field fluctuations have a typical action $E_c/\Delta \gg 1$ where the Thouless energy $E_c = D_q/q^2$ is the inverse of the classical diffusion time through the periodicity volume. This inequality is ensured by $q \ll (K/\tilde{h})^2 \sim D_q$. So, inhomogeneous fluctuations can be neglected and only the zero mode, $Q(n) \equiv Q$, is kept. Equation (20) thereby is simplified to the zero mode action,

$$S = \frac{\pi}{8\Delta}\mathrm{str}(D_q[\hat{\vartheta}, Q]^2 - 2i\omega Q\sigma^3_{\mathrm{AR}}). \quad (23)$$

Then, we substitute this action into Eq. (19). The subsequent calculations are similar to those of Ref. [22] and below we will give the results. Some details are given in Appendix A. We find

$$E(t)/(qD_q) = F(\tilde{t}), \quad \tilde{t} = t/q. \quad (24)$$

It is important that this energy profile is universal: the details of the model [e.g., the stochastic parameter K, the free Hamiltonian H_0, the denominator of rational $\tilde{h}/(4\pi)$, etc.] only determine the scales of energy and time. The explicit form of the universal function $F(\tilde{t})$ depends on the system's symmetry and is given as follows:

• For H_0 with inversion symmetry so that the quantum system reduced to a unit cell is orthogonal, we find (see Appendix A for derivations)

$$F(\tilde{t}) = \frac{1}{8}\int_1^\infty d\lambda_1 \int_1^\infty d\lambda_2 \int_{-1}^1 d\lambda \delta(2\tilde{t} + \lambda - \lambda_1\lambda_2) \times \frac{(1-\lambda^2)(1-\lambda^2-\lambda_1^2-\lambda_2^2+2\lambda_1^2\lambda_2^2)^2}{(\lambda^2+\lambda_1^2+\lambda_2^2-2\lambda\lambda_1\lambda_2-1)^2}. \quad (25)$$

For short times ($\tilde{t} \ll 1$) the Dirac function in Eq. (25) implies that the integrals are dominated by $\lambda, \lambda_{1,2} \approx 1$. Therefore, we may expand $\lambda, \lambda_{1,2}$ near unity and keep the leading expansion of $F(\tilde{t})$. As a result, $F(\tilde{t} \ll 1) \sim \tilde{t}$. For long times ($\tilde{t} \gg 1$), the integrals are dominated by

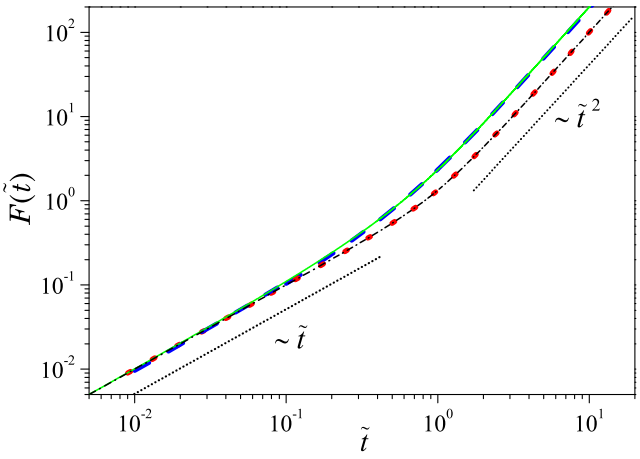

FIG. 2: (Color online) The analytical results obtained by the field theory for a generalized kicked rotor with (thick blue dashed line) and without (thick red dotted line) the inversion symmetry. It shows that the energy profile exhibits a universal crossover from metallic ($\sim \tilde{t}$) to supermetallic ($\sim \tilde{t}^2$) growth. The results are in excellent agreement with those obtained from the RMT corresponding to the orthogonal (thin green solid line) and the unitary (thin black dash-dotted line) symmetry, respectively.

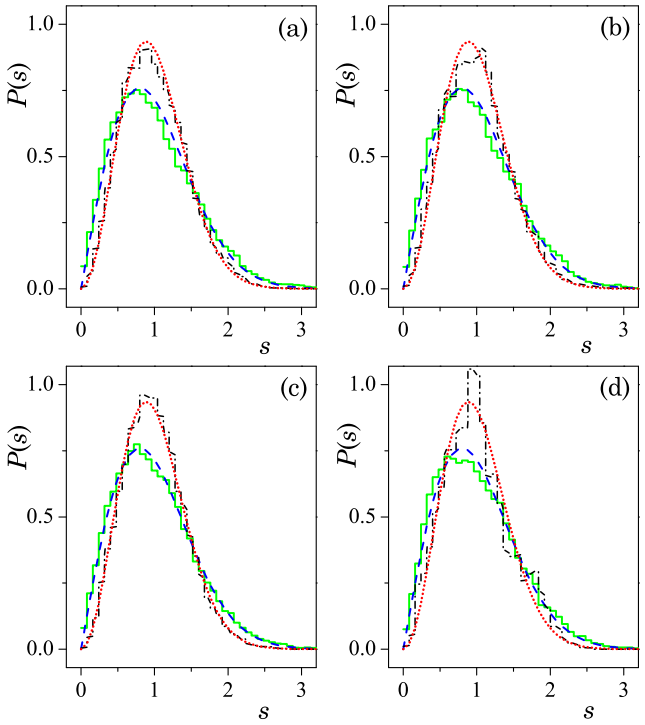

FIG. 3: (Color online) The simulation results of the distribution of the nearest level spacing $P(s)$ for $\alpha_2 = 1, \alpha_3 = 0$ (green solid histograms) and $\alpha_2 = 0, \alpha_3 = 1$ (black dash-dotted histograms) follow the Wigner-Dyson statistics for COE (blue dashed lines) and CUE (red dotted lines), respectively. The parameter $\tilde{h}/(4\pi)$ is 55/691 (a), 24/301 (b), 24/299 (c), and 7/87 (d). For all four panels $K = 300$.

$\lambda = \mathcal{O}(1)$ and $\lambda_{1,2} \gg 1$. Taking this into account we find $F(\tilde{t} \gg 1) \sim \tilde{t}^2$.

• For H_0 without the inversion symmetry so that the quantum system reduced to a unit cell is unitary, the result is the same as what has been found previously [22], which is

$$F\left(\tilde{t}\right) = \begin{cases} \tilde{t} + \frac{1}{3}\tilde{t}^3, & 0 < \tilde{t} < 1, \\ \tilde{t}^2 + \frac{1}{3}, & \tilde{t} > 1. \end{cases} \tag{26}$$

Eqs. (25) and (26) show that the energy profile exhibits a universal crossover from metallic to supermetallic growth (Fig. 2). As we will show in Sec. V, they can be obtained also from RMT.

IV. NUMERICAL TESTS

In this section we put the analytic results, namely, Eqs. (25) and (26), to numerical tests. As we will see below, although the analytical derivations of these two universal crossovers require the conditions $1 \ll K/\tilde{h} \ll q \ll (K/\tilde{h})^2$ and $K \gg 1$, they hold in broader regimes. Surprisingly, they hold even in systems (e.g., the kicked Harper system [7–9]) the quantum dynamical behaviors

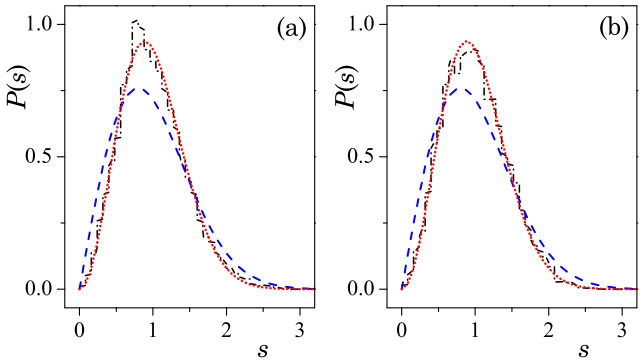

FIG. 4: (Color online) The simulation results of $P(s)$ (black dash-dotted histograms) follow the Wigner-Dyson statistics for CUE (red dotted line), as long as α_3 does not vanish. For panel (a) $\alpha_2 = 1$ and $\alpha_3 = 99$ while for (b) $\alpha_2 = 99$ and $\alpha_3 = 1$. In both cases $\tilde{h}/(4\pi) = 8/101$ and $K = 300$. The blue dashed lines are for the Wigner-Dyson statistics for COE.

of which at irrational $\tilde{h}/(4\pi)$ are fundamentally different from the standard kicked rotor [10, 11].

To numerically study the universality of the dynamics crossover we use different forms of the free Hamiltonian H_0. It has been known that this Hamiltonian, H_0, mimics "impurities" in genuine disordered systems [6, 22].

A. Polynomial-type free Hamiltonian

We first consider a polynomial-type free Hamiltonian with a specific form given by

$$H_0 = \frac{\tilde{h}^2}{2}\left(\alpha_2\hat{n}^2 + \alpha_3\hat{n}^3\right), \tag{27}$$

with $\alpha_{2,3} \in \mathbb{N}$. The $\hat{T}_i$ symmetry is present for vanishing α_3 and otherwise broken.

1. *Spectral statistics*

For a given Bloch angle θ we numerically diagonalize the Floquet operator $\hat{U}_\theta$ to obtain the quasienergy spectrum $\{\epsilon_\alpha(\theta)\}$. We repeat the computation for 1000 randomly selected values of θ so that a large ensemble is realized. We calculate the distribution of the nearest level spacing, $P(s)$, for various parameters of $\alpha_{2,3}, K$ and $\tilde{h}$. We find that $P(s)$ follows the Wigner-Dyson statistics for COE for vanishing α_3 (Fig. 3, green solid histograms) and CUE for vanishing α_2 (Fig. 3, black dash-dotted histograms). More generally, as long as $\alpha_3 \neq 0$, $P(s)$ follows the Wigner-Dyson statistics for CUE (Fig. 4). These results indicate that the system is strongly chaotic so that the field theory is expected to be valid.

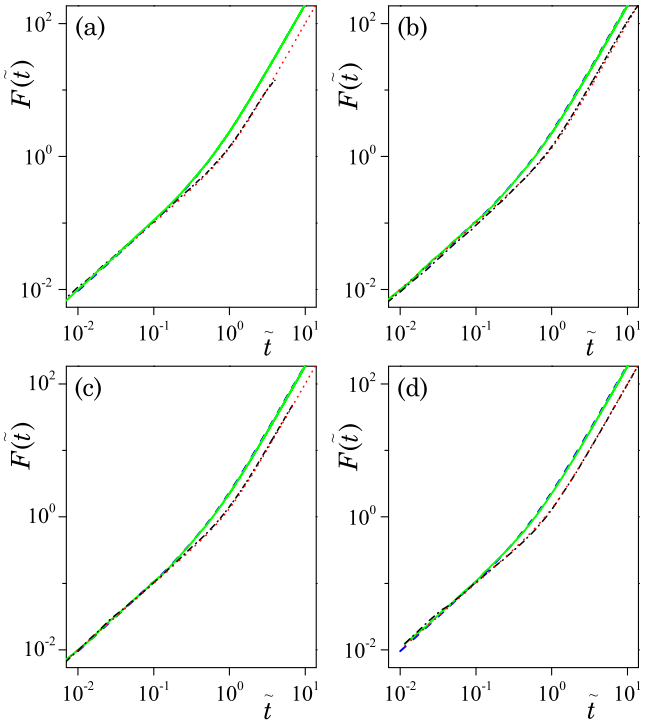

FIG. 5: (Color online) The simulation results of the rescaled energy growth $F(\tilde{t})$ for $\alpha_2 = 1, \alpha_3 = 0$ (green solid lines) and $\alpha_2 = 0, \alpha_3 = 1$ (black dash-dotted lines) convincingly support the analytic predictions for orthogonal (blue dashed lines) and unitary (red dotted lines) systems, respectively. The parameters for each panel are the same as in Fig. 3.

2. *Universal energy growth*

For a given free Hamiltonian H_0, we use the standard fast Fourier transform technique to simulate the quantum evolution (4) to compute $E(t)$ defined by Eq. (11) and in turn $F(\tilde{t})$ by Eq. (24). Fig. 5 presents the simulation results of $F(\tilde{t})$ for the free Hamiltonian H_0 given by Eq. (27) with the same parameters as in Fig. 3 for the sake of comparison. We find that for vanishing α_3 where the $\hat{T}_i$ symmetry is present, $F(\tilde{t})$ is in excellent agreement with the analytic result given by Eq. (25), while for vanishing α_2 where the $\hat{T}_i$ symmetry is broken, $F(\tilde{t})$ is in excellent agreement with the analytic result given by Eq. (26). We also find that the universal metallic-supermentallic growth crossovers (25) and (26) are valid not only in the regime of $K/\tilde{h} \ll q \ll (K/\tilde{h})^2$ (Fig. 5(a)), but also of $q \lesssim K/\tilde{h}$ (Fig. 5(b)-(d)). In addition, as shown in Fig. 6, as long as $\alpha_3 \neq 0$, for which the quasienergy spectrum follows the Wigner-Dyson statistics for CUE (see Fig. 4), the energy growth follows the metallic-supermetallic growth crossover of unitary type described by Eq. (26), confirming the sensitivity of the crossover to the system's symmetry.

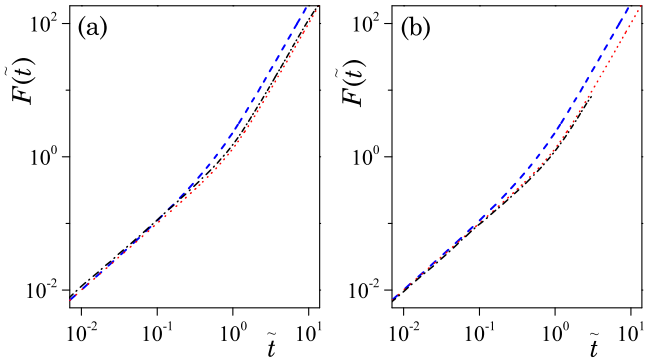

FIG. 6: (Color online) The simulation results (black dash-dotted lines) show that as long as α_3 does not vanish, $F(\tilde{t})$ follows the metallic-supermetallic growth crossover of unitary type described by Eq. (26) (red dotted lines). The parameters for each panel are the same as in Fig. 4. For comparison, the crossover of orthogonal type described by Eq. (25) (blue dashed lines) is also plotted.

B. Nonpolynomial-type free Hamiltonian

When the polynomial is of higher degree (with all coefficients being integers) but finite, we find numerically that the system's behavior at resonance remains the same. A natural question thereby arises: What happens if the degree is infinite so that H_0 is not a polynomial? To investigate this problem we consider

$$H_0 = L\cos(\tilde{h}\hat{n} + \phi). \tag{28}$$

Here L is a (nonzero) constant. When the phase parameter ϕ vanishes, this system becomes the conventional kicked Harper model [7–9] and exhibits the inversion symmetry. Whereas $\phi \neq 0$ the inversion symmetry breaks.

As shown in Fig. 7, the spectral fluctuations of the Floquet operator $\hat{U}_\theta$ obey the Wigner-Dyson statistics for COE (CUE) for $\phi = 0$ ($\pi/2$). Correspondingly, $F(\tilde{t})$ is in excellent agreement with the analytic result given by Eq. (25) for $\phi = 0$ (Fig. 8(a)) and by Eq. (26) (Fig. 8(b)) for $\phi = \pi/2$. Therefore, the analytic results for universal metal-supermetal dynamics crossover are also confirmed for the kicked Harper model.

V. DYNAMICS UNIVERSALITY FROM RMT

In this section we provide an alternative scheme for approximate analytic calculations of the energy profile. From this scheme we will see that the universality of the dynamics crossover is deeply rooted in the universal fluctuations of the Bloch's bands and eigenfunctions which are well described by the RMT. Interestingly, this scheme unveils a connection of the quantum resonance (supermetallic phase) of kicked rotors to the periodic multi-baker map [27–29].

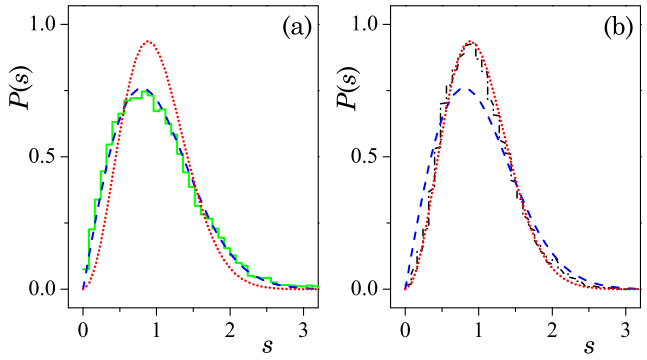

FIG. 7: (Color online) The simulation results of $P(s)$ for the kicked Harper model. The green solid histogram for $\phi = 0$ in (a) and the black dash-dotted histogram for $\phi = \pi/2$ in (b) follow the Wigner-Dyson statistics for COE (blue dashed line) and CUE (red dotted line), respectively. For both panels $\tilde{h}/(4\pi) = 24/301$ and $L = K = 300$.

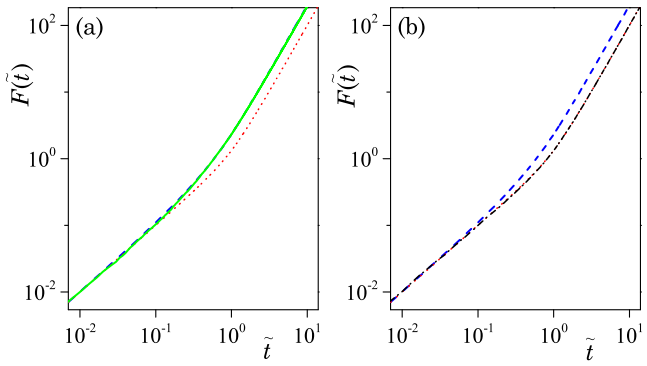

FIG. 8: (Color online) The simulation results, green solid line in (a) and black dash-dotted line in (b), of the energy growth corresponding to the two cases in Fig. 7. They exhibit again the universal metallic-supermetallic growth crossover as analytically predicted by Eq. (25) for the orthogonal (blue dashed line) and by Eq. (26) for the unitary (red dotted line) symmetry.

A. General expression of $E(t)$

To this end we compactify the angular momentum space with the periodic boundary condition so that it includes M unit cells. Recall that the initial condition is not essential. We consider the energy growth with the initial state $|\psi(0)\rangle = |\tilde{n}\rangle$ and average the energy profile with respect to $\tilde{n}$. Mathematically, this is equivalent to preparing an "equilibrium state", $\rho_{eq} = (qM)^{-1}\sum_{\tilde{n}} |\tilde{n}\rangle\langle\tilde{n}|$.

By the definition of $E(t)$ we find

$$E(t) = \frac{1}{2}\sum_{\tau_{1,2}=0}^{t-1} \mathrm{Tr}(\rho_{eq}\hat{v}(\tau_1)\hat{v}(\tau_2)) \equiv \frac{1}{2}\sum_{\tau_{1,2}=0}^{t-1} C_{\tau_1,\tau_2}, \quad (29)$$

where $\hat{v}(\tau) \equiv \frac{K}{\tilde{h}}\sin\hat{\theta}(\tau)$ may be considered as the velocity (corresponding to the motion in angular momentum space) operator, with

$$\hat{v}(\tau) = (\hat{U}^\dagger)^\tau \hat{v}\,\hat{U}^\tau, \quad (30)$$

and C_{τ_1,τ_2} is its auto-correlation function. Equation (29) is further reduced to

$$E(t) = \frac{1}{2}\left(C_0 t + 2\sum_{\tau=1}^{t-1}(t-\tau)C_\tau\right) \quad (31)$$

thanks to $C_{\tau_1,\tau_2} = C_{\tau_1-\tau_2}$.

Next, we calculate the auto-correlation function C_τ. It can be rewritten as

$$C_\tau = \left(\frac{K}{\tilde{h}}\right)^2 \frac{1}{qM}\mathrm{Tr}((\hat{U}^\dagger)^\tau \sin\hat{\theta}\hat{U}^\tau \sin\hat{\theta}) \quad (32)$$

by using its definition [cf. Eq. (29)]. Employing the Bloch's theorem (13) we obtain

$$\begin{aligned} C_\tau &= \left(\frac{K}{\tilde{h}}\right)^2 \frac{1}{qM}\sum_{\alpha,\alpha'}\sum_{\theta,\theta'} e^{-i(\epsilon_\alpha(\theta)-\epsilon_{\alpha'}(\theta'))\tau} \\ &\times |\tilde{\mathbf{J}}_{\alpha\theta,\alpha'\theta'}|^2, \quad (33) \\ \tilde{\mathbf{J}}_{\alpha\theta,\alpha'\theta'} &= \langle\psi_{\alpha,\theta}|\sin\hat{\theta}|\psi_{\alpha',\theta'}\rangle. \quad (34) \end{aligned}$$

The matrix elements of $\tilde{\mathbf{J}}$ can be simplified to

$$\begin{aligned} \tilde{\mathbf{J}}_{\alpha\theta,\alpha'\theta'} &= \frac{1}{2iM}\sum_{\tilde{n},\tilde{n}'} \varphi^*_{\alpha,\theta}(\tilde{n})\varphi_{\alpha',\theta'}(\tilde{n}')e^{i(\tilde{n}\theta-\tilde{n}'\theta')} \\ &\times (\delta_{\tilde{n}-\tilde{n}',1} - \delta_{\tilde{n}-\tilde{n}',-1}) \\ &= \frac{1}{2i}\delta_{\theta\theta'}\sum_{n=0}^{q-1}(\varphi^*_{\alpha,\theta}(n)\varphi_{\alpha',\theta}(n-1)e^{i\theta} \\ &-\varphi^*_{\alpha,\theta}(n)\varphi_{\alpha',\theta}(n+1)e^{-i\theta}) \\ &\equiv \delta_{\theta\theta'}\tilde{\mathbf{J}}_{\alpha\alpha'}(\theta). \quad (35) \end{aligned}$$

In deriving the second equality we have summed over the Bravis lattice which enforces $\theta = \theta'$. Substituting Eq. (35) into Eq. (33) gives

$$C_\tau = \left(\frac{K}{\tilde{h}}\right)^2 \frac{1}{qM}\sum_{\alpha,\alpha'}\sum_{\theta} e^{-i(\epsilon_\alpha(\theta)-\epsilon_{\alpha'}(\theta))\tau}|\tilde{\mathbf{J}}_{\alpha\alpha'}(\theta)|^2 \quad (36)$$

By setting $\tau = 0$ in Eqs. (32) and (36) we find the following identity,

$$\frac{1}{Lq}\sum_{\alpha,\alpha'}\sum_{\theta}|\tilde{\mathbf{J}}_{\alpha\alpha'}(\theta)|^2 = \frac{1}{2}. \quad (37)$$

Eqs. (31) and (36) constitute an exact formalism for calculating $E(t)$. Formally, they are identical to the formulas giving the mean-squared displacement in the periodic multi-baker map. The latter essentially is composed of an infinite number of standard baker's maps, which are coupled to each other, with the coupling being spatially periodic [35]. (The details are certainly not.)

B. Effects of chaotic fluctuations of Bloch bands and wave functions

Equation (36) shows that the correlation is governed by the quasienergy spectrum $\{\epsilon_\alpha(\theta)\}$ and the corresponding eigenfunctions $\varphi_{\alpha,\theta}$, which determine the oscillatory factor $e^{-i(\epsilon_\alpha(\theta)-\epsilon_{\alpha'}(\theta))\tau}$ and the matrix elements of the velocity operator, i.e., $\tilde{\mathbf{J}}_{\alpha\alpha'}(\theta)$, respectively. Because the reduced quantum system in a unit cell (for given Bloch angle θ) is chaotic, both $\{\epsilon_\alpha(\theta)\}$ and $\varphi_{\alpha,\theta}$ exhibit chaotic fluctuations. If we assume that the fluctuations of $\{\epsilon_\alpha(\theta)\}$ and $\varphi_{\alpha,\theta}$ are independent, then the correlation function is simplified to

$$C_\tau \to \left(\frac{K}{\tilde{h}}\right)^2 \frac{1}{Lq}\sum_{\alpha,\alpha'}\sum_{\theta}\left\langle e^{-i(\epsilon_\alpha(\theta)-\epsilon_{\alpha'}(\theta))\tau}\right\rangle \times\left\langle |\tilde{\mathbf{J}}_{\alpha\alpha'}(\theta)|^2\right\rangle, \tag{38}$$

where $\langle\cdot\rangle$ stands for the averages over a random ensemble of energy spectrum and wave functions, respectively. These random ensembles are well described by the RMT.

For the system without the inversion symmetry ($\beta = 2$), following Ref. [29] we use the RMT corresponding to CUE to find

$$\left\langle e^{-i(\epsilon_\alpha(\theta)-\epsilon_{\alpha'}(\theta))\tau}\right\rangle = \begin{cases} 1, & \tau = 0; \\ \frac{\tau-q}{q(q-1)}, & 0<\tau<q; \\ 0. & \tau \geq q. \end{cases} \tag{39}$$

For the system with the inversion symmetry ($\beta = 1$), we find

$$\left\langle e^{-i(\epsilon_\alpha(\theta)-\epsilon_{\alpha'}(\theta))\tau}\right\rangle = \begin{cases} 1,\ \tau = 0; \\ \frac{1}{q(q-1)}\left(-q+2\tau\left(f(\frac{q}{2}+\tau)-f(\frac{q}{2})\right)\right),\ 0<\tau<q; \\ \frac{1}{q(q-1)}\left(-q+2\tau\left(f(\frac{q}{2}+\tau)-f(\tau-\frac{q}{2})\right)\right),\ \tau\geq q \end{cases} \tag{40}$$

corresponding to COE, where $f(\tau)\equiv\sum_{k=1}^{\tau}\frac{1}{2k-1}$. Note that these results are independent of θ.

We cannot calculate the second factor in Eq. (38) analytically. Instead, motivated by the similarity between Eq. (36) and the corresponding expression for the periodic multi-baker map, we hypothesize that the matrix elements of the velocity operator have the universal behavior. So, we translate the results of Ref. [29] obtained from the RMT to the present context which read

$$\left\langle |\tilde{\mathbf{J}}_{\alpha\alpha'}(\theta)|^2\right\rangle = \begin{cases} \frac{1}{2}\frac{3-\beta}{q+3-\beta}, & \alpha=\alpha'; \\ \frac{1}{2}\frac{q}{(q-1)(q+3-\beta)}, & \alpha\neq\alpha', \end{cases} \tag{41}$$

where the overall factor of $1/2$ makes it obey the identity (37). Below key predictions obtained from this ansatz are confirmed.

We substitute Eqs. (39)-(41) into Eq. (38). In combination with Eq. (31) we obtain for $\beta = 1$ ($D_q = (\frac{K}{2\tilde{h}})^2$)

$$\frac{E(t)}{qD_q} = \begin{cases} \tilde{t}+\frac{\tilde{t}(\tilde{t}-q^{-1})}{(1+2q^{-1})}\left(1+\frac{\tilde{t}-2q^{-1}}{3(1-q^{-1})}\right), & 0<\tilde{t}<1; \\ \frac{2\tilde{t}^2}{1+2q^{-1}}+\frac{1+q^{-1}}{3(1+2q^{-2})}, & \tilde{t}\geq 1, \end{cases} \tag{42}$$

where small corrections have been ignored, and for $\beta = 2$

$$\frac{E(t)}{qD_q} = \begin{cases} \tilde{t}+\frac{\tilde{t}(\tilde{t}-q^{-1})(\tilde{t}-2q^{-1})}{3(1-q^{-2})}, & 0<\tilde{t}<1; \\ \frac{\tilde{t}^2}{1+q^{-1}}+\frac{1}{3}, & \tilde{t}\geq 1. \end{cases} \tag{43}$$

As shown in Fig. 2, these results are in excellent agreement with those predicted by the field theory and are confirmed by simulations as shown in Sec. IV. Indeed, for $\beta = 2$, Eq. (43) is identical to the analytic expression (26) for $q \gg 1$. Equations (42) and (43) show that

$$\frac{E|_{\beta=1}(t)}{E|_{\beta=2}(t)} \xrightarrow{t\gg 1} 2, \quad \text{for } q\gg 1. \tag{44}$$

Summarizing, the universal metal-supermetal dynamics crossover can be attributed to universal chaotic fluctuations of Bloch bands and eigenfunctions. Since the latter are well described by the RMT, we expect that such dynamics universality is identical to the RMT universality. On the other hand, it is well known [36] that very rich RMT universality classes are brought about by different symmetries. Although in this work only crossovers corresponding to the orthogonal and unitary classes are found, the richness of RMT universality classes implies that even richer universal crossover behaviors may exist, provided the system exhibits other symmetries.

VI. CONCLUSION

We analytically and numerically studied the dynamics of a large class of generalized kicked rotor systems the Hamiltonian of which is given by Eq. (2) with rational $\tilde{h}/(4\pi) = p/q$. The universal laws for the crossover from metal to supermetal dynamics are found, manifesting themselves in universal crossovers from metallic (linear) to supermetallic (quadratic) energy growth. These crossover behaviors are determined only by the system's symmetry and insensitive to the details such as the values of p and q and the strength of the kicking potential which only affect the energy and the time scales. Specifically, we find that when the Hamiltonian $H_0(\hat{n})$ governing the free rotation has inversion symmetry, i.e., $H_0(\hat{n}) = H_0(-\hat{n})$, the energy profile follows an orthogonal-type crossover behavior, described by Eq. (25), and otherwise the crossover is a unitary type, described by Eq. (26). We show by the RMT that these universal dynamics crossovers can be attributed to the universal Bloch wave functions and band fluctuations of quantum systems reduced to a unit cell. This leads us to conjecture that in more general chaotic systems with periodic driving, the universality class of the

metal-supermetal dynamics crossover is identical to that of eigenfunction and spectral fluctuations described by the RMT.

Our results can be generalized to condensed-matter systems (such as semiconductors) where Bloch bands have been seen to exhibit chaotic fluctuations following the RMT. For these systems even richer universality classes have been predicted [36]. The ensuing metal-supermetal dynamics crossovers are expected to fall into different universality classes manifesting in different universal behaviors of the optical conductivity. Provided the unit cell is so complicated that the Bloch energy spectrum exhibits chaotic fluctuations following the Wigner-Dyson statistics, our results are expected to be valid.

Finally, we remark that in Ref. [21] the supermetallic growth has been rigorously established for the standard kicked rotor under general parametric conditions. This result was obtained without resorting to the chaoticity condition. A byproduct of the present work, i.e., $E(t \to \infty) \sim t^2$, is consistent with this rigorous result, but is established based on the chaoticity condition. We believe that our main result of universal metal-supermetal dynamics crossovers is of chaos origin. Such a crossover phenomenon was not studied in Ref. [21].

Acknowledgements

This work is supported by the National Natural Science Foundation of China (Grant Nos. 11174174, 11275159, 11335006, and 11535011).

Appendix A: Derivations of Eq. (25)

In this Appendix we derive Eq. (25). To this end we employ the polar coordinate representation of Q [37]. Specifically, we parametrize Q as

$$Q = RQ_0R^{-1}, \quad Q_0 = \begin{pmatrix} \cos\hat{\Theta} & i\sin\hat{\Theta} \\ -i\sin\hat{\Theta} & -\cos\hat{\Theta} \end{pmatrix}_{\rm AR}, \quad \text{(A1)}$$

where Q_0 is the radial part and

$$\hat{\Theta} = \begin{pmatrix} \hat{\theta}_{11} & 0 \\ 0 & \hat{\theta}_{22} \end{pmatrix}_{\rm BF}, \quad \text{(A2)}$$
$$\hat{\theta}_{11} = \begin{pmatrix} \tilde{\theta} & 0 \\ 0 & \tilde{\theta} \end{pmatrix}_{\rm T}, \quad \hat{\theta}_{22} = i\begin{pmatrix} \tilde{\theta}_1 & \tilde{\theta}_2 \\ \tilde{\theta}_2 & \tilde{\theta}_1 \end{pmatrix}_{\rm T}$$

with $0 < \tilde{\theta} < \pi, \tilde{\theta}_{1,2} > 0$, and R is the transverse part commuting with $\sigma^3_{\rm AR}$. It is important to note that the Grassmann variables enter only into R (see Ref. [37] for details).

We substitute this parametrization into Eqs. (19) and (23). Taking into account that Eq. (21) now is simplified to

$$\hat{\vartheta} = \begin{pmatrix} \theta_+ & 0 \\ 0 & \theta_- \end{pmatrix}_{\rm AR} \otimes \sigma^0_{\rm T} \otimes \sigma^0_{\rm FB}, \quad \text{(A3)}$$

we find

$$K_\omega = \frac{1}{4}\int_1^\infty d\lambda_1 \int_1^\infty d\lambda_2 \int_{-1}^1 d\lambda\, e^{-S} \times \frac{(1-\lambda^2)(1-\lambda^2-\lambda_1^2-\lambda_2^2+2\lambda_1^2\lambda_2^2)}{(\lambda^2+\lambda_1^2+\lambda_2^2-2\lambda\lambda_1\lambda_2-1)^2}, \quad \text{(A4)}$$

where the radial coordinates $\lambda \equiv \cos\tilde{\theta}, \lambda_{1,2} \equiv \cosh\tilde{\theta}_{1,2}$ and the zero-mode action

$$S = \frac{\pi}{2\Delta}[D_q(\Delta\theta)^2(2\lambda_1^2\lambda_2^2-\lambda^2-\lambda_1^2-\lambda_2^2+1) + 2i\omega(\lambda-\lambda_1\lambda_2)]. \quad \text{(A5)}$$

Substituting Eq. (A4) into Eq. (16) we obtain Eq. (25).

[1] G. Casati, B. V. Chirikov, J. Ford, and F. M. Izrailev, in *Stochastic Behavior of Classical and Quantum Hamiltonian Systems*, Lecture Notes in Physics **93**, edited by G. Casati and J. Ford (Springer, New York, 1979).
[2] F. M. Izrailev, Phys. Rep. **196**, 299 (1990).
[3] B. Chirikov and D. Shepelyansky, Scholarpedia **3**, 3550 (2008).
[4] S. Fishman, Scholarpedia **5**, 9816 (2010).
[5] B. V. Chirikov, Phys. Rep. **52**, 263 (1979).
[6] S. Fishman, D. R. Grempel and R. E. Prange, Phys. Rev. Lett. **49**, 509 (1982).
[7] G. M. Zaslavskii, M. Yu. Zakharov, R. Z. Sagdeev, D. A. Usikov, and A. A. Chernikov, Sov. Phys. -JETP **64**, 294 (1986).
[8] P. Leboeuf, J. Kurchan, M. Feingold, and D. P. Arovas, Phys. Rev. Lett. **65**, 3076 (1990).
[9] T. Geisel, R. Ketzmerick, and G. Pestchel, Phys. Rev. Lett. **67**, 3635 (1991).
[10] R. Lima and D. Shepelyansky, Phys. Rev. Lett. **67**, 1377 (1991).
[11] J. Wang and J. Gong, Phys. Rev. A **77**, 031405(R) (2008).
[12] C. Tian, A. Altland, and M. Garst, Phys. Rev. Lett. **107**, 074101 (2011); J. Wang, C. Tian, and A. Altland, Phys. Rev. B **89**, 195105 (2014).
[13] D. Y. H. Ho and J. Gong, Phys. Rev. Lett. **109**, 010601 (2012).
[14] H. Wang, L. Zhou, and J. Gong, Phys. Rev. B **91**, 085420 (2015).
[15] J. Wang, I. Guarneri, G. Casati, and J. B. Gong, Phys.

Rev. Lett. **107**, 234104 (2011).
[16] Y. Chen and C. Tian, Phys. Rev. Lett. **113**, 216802 (2014).
[17] F. M. Izrailev and D. L. Shepelyansky, Teor. Mat. Fiz. **43**, 417 (1980) [Teor. Math. Phys. **43**, 553 (1980)].
[18] G. Casati and I. Guarneri, Commun. Math. Phys. **95**, 121 (1984).
[19] I. Dana, E. Eisenberg, and N. Shnerb, Phys. Rev. E **54**, 5948 (1996); I. Dana and D. L. Dorofeev, Phys. Rev. E **73**, 026206 (2006).
[20] S. Wimberger, I. Guarneri, and S. Fishman, Nonlinearity **16**, 1381 (2003).
[21] I. Guarneri, Ann. Henri Poincaré **10**, 1097 (2009).
[22] C. Tian and A. Altland, New J. Phys. **12**, 043043 (2010).
[23] M. Sadgrove and S. Wimberger, Adv. At. Mol. Opt. Phys. **60**, 315 (2011).
[24] S. Zhdanovich, C. Bloomquist, J. Floβ, I. Sh. Averbukh, J. W. Hepburn, and V. Milner, Phys. Rev. Lett. **109**, 043003 (2012).
[25] N. Taniguchi and B. L. Altshuler, Phys. Rev. Lett. **71**, 4031 (1993).
[26] C. Tian, Phys. Rev. Lett. **102**, 243903 (2009).
[27] D. K. Wójcik and J. R. Dorfman, Phys. Rev. E **66**, 036110 (2002).
[28] D. K. Wójcik and J. R. Dorfman, Phys. Rev. Lett. **90**, 230602 (2003).
[29] D. K. Wójcik and J. R. Dorfman, Physica D **187**, 223 (2004).
[30] E. P. Wigner, SIAM Rev. **9**, 1 (1967).
[31] N. W. Aschroft and N. D. Mermin, *Solid state physics* (Harcourt college publishers, Fort Worth, 1976).
[32] This symmetry is unimportant for irrational $\tilde{h}/(4\pi)$.
[33] Exactly speaking, $E(t)$ such defined is the second moment of the wavepacket, and thus characterizes the wavepacket spreading. It gives the genuine kinetic energy only for quadratic H_0. Here we follow the convention to call it kinetic energy.
[34] We do not study the role of classical anomalies, such as accelerator mode (G. M. Zaslavsky, M. Edelman, and B. A. Niyazov, Chaos **7**, 159 (1997)) in the standard kicked rotor occurring at special values of K.
[35] See Eqs. (17) and (22) in Ref. [29].
[36] A. Altland and M. R. Zirnbauer, Phys. Rev. B **55**, 1142 (1997).
[37] K. B. Efetov, *Supersymmetry in disorder and chaos* (Cambridge, UK, 1997).